Spreading of rinsing liquids across a horizontal rotating substrate

Daniel J. Walls, Andrew S. Ylitalo, David S. L. Mui, John M. Frostad, and Gerald G. Fuller

Phys. Rev. Fluids **4**, 084102 — Published 7 August 2019

DOI: 10.1103/PhysRevFluids.4.084102

Spreading of rinsing liquids across a horizontal, rotating substrate

Daniel J. Walls,[1,2,*] Andrew S. Ylitalo,[1,3,*] David S. L. Mui,[4] John M. Frostad,[1,2,5,†] and Gerald G. Fuller[1,‡]
[1]*Department of Chemical Engineering, Stanford University, Stanford, California 94305, United States*
[2]*Department of Chemical and Biological Engineering, University of British Columbia, Vancouver, British Columbia V6T 1Z3, Canada*
[3]*Division of Chemistry and Chemical Engineering, California Institute of Technology, Pasadena, CA 91125, United States*
[4]*Lam Research Corporation, Fremont, California 94538, United States*
[5]*Food Science, University of British Columbia, Vancouver, British Columbia V6T 1Z3, Canada*

"Rinsing" liquids and their dynamics are interesting both fundamentally in the interaction of several classic modes of spreading, and industrially in a variety of cleaning applications, such as in the manufacturing of silicon wafers. In this paper, we investigate the time-dependent spreading behavior of a rinsing liquid across a horizontal, rotating substrate; the rinsing liquid is applied to the center of the rotating substrate as an orthogonal impinging jet of constant volumetric flow. We present experimental findings on the azimuthally averaged outer radius of the spreading liquid, in which we observed four distinct growth behaviors in time. We use lubrication theory to explain these phenomena and to define boundaries within the explored parameter space where each was observed. In the absence of rotation, capillarity dominates and the spreading radius grows as $t^{4/10}$. When centrifugal forces dominate the spreading process, several time dependencies of the spreading radius are possible, with lubrication theory predicting exponential growth as well as power laws of $t^{3/4}$ and $t^{3/2}$.

I. INTRODUCTION

The spreading of liquids across solid surfaces is a classic problem in fluid mechanics [1]. In this paper, we study the time-dependent spreading behavior of a "rinsing" liquid across a horizontal, rotating substrate through experiment and theory, with the rinsing liquid applied to the center of the rotating substrate as an orthogonal impinging jet of constant volumetric flow. The dynamics of the spreading of rinsing liquids are important both fundamentally as well as from an industrial perspective, where rinsing liquids are used to clean surfaces both gently and thoroughly; hence, the name "rinsing" liquids. To build a fundamental understanding of these dynamics, we consider three modes of spreading that have been examined previously on horizontal surfaces—capillary, gravitational, and centrifugal [2–23]—and the dynamics of impinging liquid jets and hydraulic jumps [24–35].

Capillary spreading of sessile droplets across horizontal substrates was first studied by Voinov [2], Tanner [3], and Cox [4] using lubrication theory and experiments. These researchers determined that features of the drop, such as radius, height, and contact angle, evolved following power laws in time. Similarly, early studies of gravitational spreading of fixed volumes and constant flows of liquid by Didden and Maxworthy [5] and Huppert [6] found power-law behaviors in time as well. The dominant mechanism of spreading between capillarity and gravity is determined using the Bond number [36]. In the wake of these pioneering studies, a vast quantity of work has been produced [7–12], and Craster and Matar have compiled a comprehensive review [13].

An early theoretical study of centrifugal spreading of fixed volumes of liquid across horizontal substrates was reported by Emslie *et al.* [14]. Later, Melo *et al.* [15] conducted an experimental study of fixed volumes of silicone oils spreading across a horizontal, rotating substrate. The authors noted that the liquid initially spread axisymmetrically and utilized lubrication theory to explain the spreading behavior. At a critical radius, fingers (rivulets) would develop and propagate, breaking the axisymmetry of the liquid spreading front; the authors were able to compare the observed onset of the instability to a linear stability analysis of driven spreading films by Troian *et al.* [16]. Fraysse and Homsy [17] conducted a similar study, extending their investigation to include Boger liquids as well as modulating the wetting properties of the substrate. No difference was observed in the onset of the instability with the selected Boger fluid, however, liquids that better wet the substrate were observed to spread to a larger critical radius before rivulets developed. Two subsequent papers by Spaid and Homsy [18, 19] further investigated the effect of elasticity on the onset and development of the fingering instability with experiments and theory, concluding that sufficiently elastic liquids delay the onset of the instability to larger critical radii. Wilson *et al.* [20] sought to explain the experimental observations of Fraysse and Homsy [17] and Spaid and Homsy [19], approaching the problem of a fixed volume of liquid spreading due to centrifugal forces with numerical calculations as well as analytically with zero and asymptotically weak surface tension. In two reports, McKinley *et al.* [21, 22] also used numerical and analytical approaches in studying the axisymmetric instabilities (rather than rivulets discussed earlier) that develop in a fixed volume of liquid on either a rotating substrate or subjected to an impinging jet of air, with the authors demonstrating their equivalence. More recently, Holloway *et al.* [23] focused on the growth of rivulets and its dependence on the rotation rate and volume of the spreading droplet. These authors have individually noted the limitations of their analyses in describing the spreading radius once rivulets formed.

The aforementioned studies of centrifugal spreading did not consider an impinging source of a constant volumetric flow of liquid, which is a typical mechanism for applying a rinsing liquid to a surface. Hsu *et al.* [24] and Walker *et al.* [25] used impinging liquids to rinse a thin layer of another miscible liquid from a non-rotating surface. As the rinsing liquid impinged upon the surface, it produced a hydraulic jump that propagated radially outward, ideally sweeping away the thin layer of the miscible liquid. These investigations built upon earlier studies of stationary hydraulic jumps first presented by Rayleigh [26], and later addressed in a seminal paper by Watson [27] with experimental and theoretical analyses that demonstrated the effect of viscosity. An array of work has followed on hydraulic jumps [28–34], and a review of many studies can be found in Bush and Aristoff [35].

Here, however, we do not study hydraulic jumps produced by impinging liquid jets, but rather the spreading of the liquids applied by the jets. Considering the prior work, we investigate the rate of spreading of rinsing liquids applied to horizontal, rotating substrates by a central, impinging jet of constant volumetric flow. We observed several distinct behaviors in time for the growth of the azimuthally averaged radius of the spreading front, or spreading radius, throughout the explored parameter space. We develop a theoretical description of each observed spreading behavior using lubrication theory. As the focus of this paper is the growth of the azimuthally averaged spreading radius, we refrain from discussing rivulets explicitly here, except in formulating our theoretical assumptions to reflect the character of the spreading behavior. A companion paper by Ylitalo *et al.* [37] contains a detailed discussion of the rivulets observed in these experiments, and their formation, growth, and morphologies.

II. EXPERIMENT

Figure 1 shows a schematic diagram of the experimental apparatus constructed to permit high-speed recording of a rinsing liquid impinging upon, and spreading across, a horizontal, rotating substrate. The circular substrate was mounted onto the chuck of a spin coater (Lam Research) by six spring-loaded pins spaced equally along its circumference. A nozzle with an inner diameter of 6.35 mm was positioned 4 cm above the center of the substrate to orthogonally apply an impinging jet of rinsing liquid to the substrate. Rinsing liquid was pumped at a constant flow rate through the nozzle by a digital gear pump (Cole-Parmer, Micropump L20562 and Digital Drive 75211-30). A high density polyethylene (HDPE) shield encircled the substrate to collect liquid runoff. A high-speed camera (Photron, FASTCAM SA3 Model 120K) was positioned off-center and at an angle to allow a direct line of sight to the center of the substrate. The aperature of the camera lens (Edmund Optics, 25 mm F1.4) was adjusted to increase the depth of focus such that the surface of the substrate as well as the reflection of a patterned background held above the apparatus were simultaneously in focus. The patterned background enhances the visibility of the spreading front of the rinsing liquid. Four 250 W halogen lamps were directed upwards at the patterned background to illuminate the substrate. The lamps were connected to the alternating current of the laboratory through a custom-built rectifying electrical circuit to sufficiently dampen the typical light flickering observed when recording images at high frame rates. The circuit consisted of a rectifier bridge (Diodes Incorporated, GBJ-2004-F), an electrolytic capacitor (EPCOS/TDK, B43456-A9338-M), and a thermistor (Ametherm, SL32 5R020).

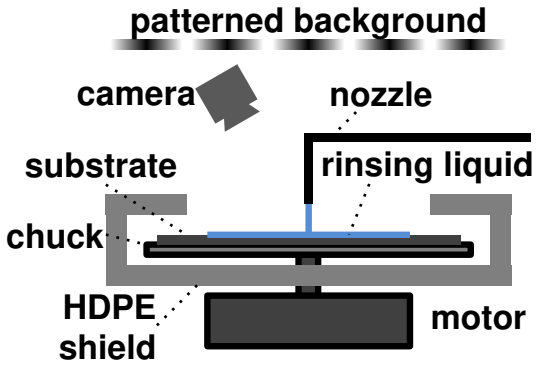

FIG. 1: Schematic diagram of the experimental apparatus. A circular substrate is mounted onto the chuck of a spin coater (Lam Research). A nozzle is positioned above the center of the substrate to orthogonally apply an impinging jet of rinsing liquid to the substrate. A high density polyethylene (HDPE) shield encircles the substrate to collect liquid runoff. A patterned background is positoned above the substrate. A high-speed camera images the spreading of the rinsing liquid.

Rinsing experiments were conducted on a 300-mm-diameter silicon wafer (Lam Research). Prior to a rinsing experiment, the surface of the substrate was either uncoated (bare) or coated with a thin liquid layer. When present, the thin coating layer was applied just prior to the rinsing experiment by spin coating 30 mL of the desired coating liquid across the substrate to a thickness of approximately 15 μm, following the theoretical developments of Emslie

et al. [14]. During a rinsing experiment, the impinging jet of rinsing liquid was applied orthogonally at the center of the rotating substrate until it completely covered the substrate. At the conclusion of each experiment, the rotating substrate was dried using compressed air.

Flow rate of the rinsing liquid, Q, was varied between 840 and 2860 mL/min. Rotation rate of the substrate, Ω, was varied between 0 and 1000 rev/min. Deionized water was used as the rinsing liquid. Deionized water and aqueous solutions of 3 mM sodium dodecylsulfate (SDS, Invitrogen Life Technologies) surfactant were used as coating liquids. SDS is a commonly studied, anionic surfactant that is electrostatically repelled from the negatively charged silicon substrate. Experiments using concentrations of SDS at and above its critical micelle concentration (6.5 mM and 10 mM, respectively) were conducted, but are not reported here as they elicited similar behavior to the 3 mM SDS solution.

Additional details on the apparatus, cleaning procedures, and image processing are reported in the companion paper by Ylitalo *et al.* [37].

III. RESULTS AND DISCUSSION

We observed four distinct behaviors in time for the growth of the spreading radius throughout the explored parameter space of rotation rate, flow rate, and coating layer. On bare and SDS-coated substrates, three distinct time-dependent spreading behaviors were found; Figure 2 qualitatively shows the three corresponding regions where a single spreading behavior was observed across the entire substrate after the initial impingement of the rinsing liquid with respect to the rotation and flow rates. We consider these experiments before returning to those on water-coated substrates, where a fourth region was observed. In Region 1 (narrow horizontal band in light gray), the rotation of the substrate is relatively slow such that centrifugal forces are insignificant and only capillarity or gravity can lead to spreading. As rotation is increased, centrifugal forces become consequential, and the dynamics transition into Region 2 (medium gray), and at lower flow rates, Region 3 (dark gray). Additionally, there are several experiments where one distinct time-dependent behavior was not evident, particularly between Regions 1 and 2 with the transition between capillary and centrifugal spreading. We will discuss each set of experiments in turn, starting with those of Region 2 where exponential growth of the spreading radius was observed.

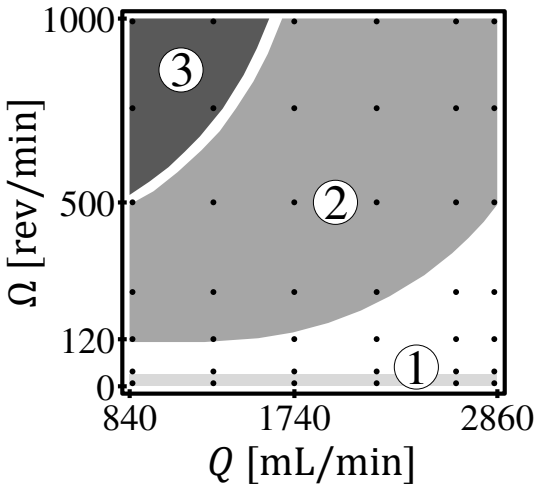

FIG. 2: A sketch of three regions corresponding to the three time-dependent spreading behaviors observed on bare and SDS-coated substrates with respect to flow and rotation rates: (1) capillary (power law), (2) centrifugal (exponential), and (3) centrifugal (power law). Dots indicate the selected flow and rotation rates of individual experiments.

Figure 3a shows a plot of the azimuthally averaged spreading radius, r_N, as a function of time for a rinsing experiment on a bare substrate within Region 2 (Q = 1290 mL/min, Ω = 120 rev/min). The data are plotted on logarithmic(radius)-linear(time) axes, where a linear response indicates an exponential process. The spreading radius grows exponentially after initial splashing from the impingement of the rinsing liquid on the substrate, with a time constant inversely proportional to the rotation rate. Arrows indicate points in the experiment corresponding to the concentric outlines of the spreading front (right inset); gaps in the outlines occur where the view of the spreading front was obstructed by the jet nozzle.

To explain the observed exponential growth of the spreading radius in this region, we employ lubrication theory in cylindrical coordinates, defining the axial and lateral length scales, $l_{c,z}$ and l_c, as a characteristic thickness and radius of the rinsing liquid, respectively. A standard lubrication treatment discards all inertial terms because the

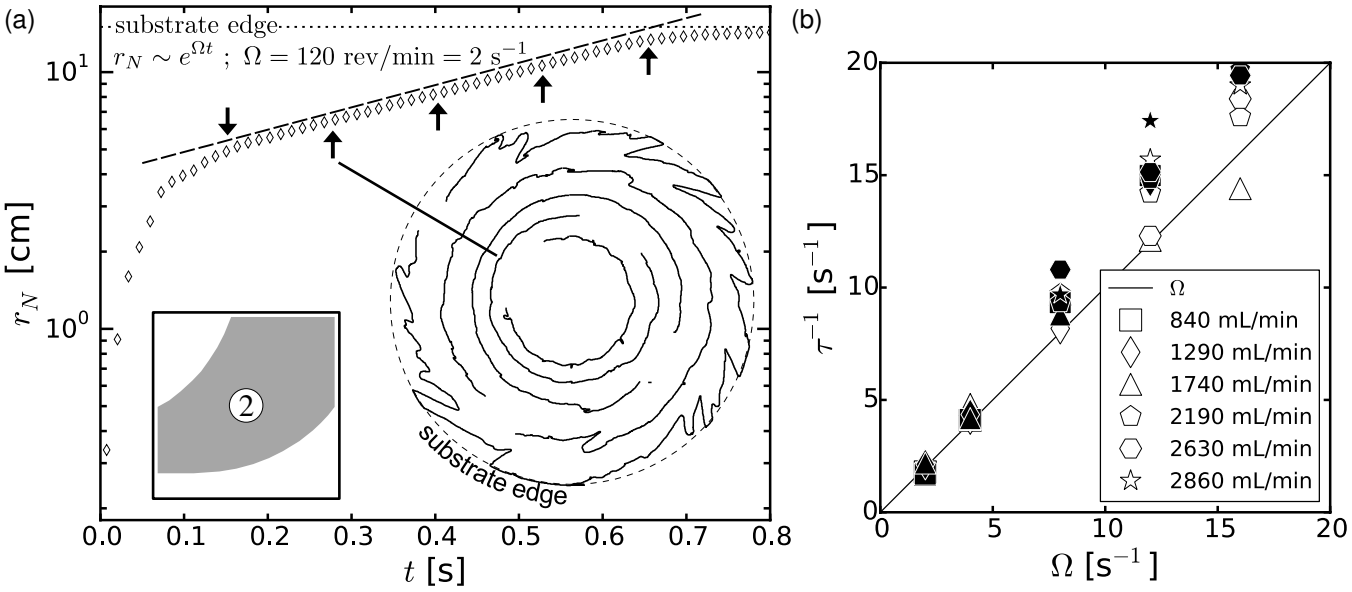

FIG. 3: (a) Plot of measurements of the azimuthally averaged spreading radius as a function of time for a rinsing liquid (water) spreading across a bare substrate (Q = 1290 mL/min, Ω = 120 rev/min = 2 s^{-1}). Symbols depict experimental measurements. Dashed and dotted lines indicate exponential growth and the edge of the substrate, respectively. Arrows indicate points corresponding to the concentric outlines of the spreading front (right inset). (b) Plot of the inverses of measured time constants of exponential growth, τ^{-1}, against rotation rate, Ω, for each observation of exponential growth. Open and filled symbols indicate bare and SDS-coated substrates, respectively.

ratio of these length scales is very small, $l_{c,z}/l_c = \epsilon \ll 1$, and by extension $\epsilon^2 Re \ll 1$, where $Re = \rho u_c l_c/\mu$ is the Reynolds number with u_c as the characteristic velocity and ρ and μ as the density and viscosity of the rinsing liquid, respectively. However, conditions similar to the experiments shown in Figure 3 ($l_c \sim 0.1$ m, $l_{c,z} \sim 0.001$ m, and $u_c = \Omega l_c \sim 1$ m/s) give $\epsilon^2 Re \sim O(1)$ and greater. Thus, inertia is not negligibly small. Retaining these terms gives the dimensionless equation for the conservation of radial momentum as

$$\epsilon^2 Re\left(u_r' \frac{\partial u_r'}{\partial r'} + u_z' \frac{\partial u_r'}{\partial z'}\right) = -\frac{\epsilon^2 l_c p_c}{\mu u_c}\frac{\partial p'}{\partial r'} + \frac{\partial^2 u_r'}{\partial z'^2}, \tag{1}$$

where u_r' and u_z' are the velocities in the radial and axial directions, respectively, and p' and p_c are the pressure and characteristic pressure, respectively. A prime, $'$, denotes a dimensionless variable. Both Batchelor [38] and Leal [36] utilized inertial lubrication in investigating the centrifugal flow due to a rotating disk in a semi-infinite fluid and the levitation of an air hockey puck, respectively. Here, however, the semi-infinite solution reported by Batchelor does not transpose directly onto the present problem due to the free interface as the upper boundary. Thus, we proceed by defining the height of the rinsing liquid as $h'(r',t')$ and seeking an approximate solution for the spreading radius of the rinsing liquid using the height-averaged radial velocity, $\bar{u}_r'$, where $\bar{u}_r' h' = \int_0^{h'(r',t')} u_r' dz'$. In a rotational reference frame, centrifugal force emerges through pressure, taking the form of $p' = p^{*\prime} - \rho\Omega^2 l_c^2 r'^2/2p_c$, where $p^{*\prime}$ is a reference pressure. Using $\bar{u}_r'$, p', and u_c simplifies Equation (1) to

$$\bar{u}_r' \frac{\partial \bar{u}_r'}{\partial r'} = r'. \tag{2}$$

Noting that radial velocity is the time derivative of the radius, Equation (2) can be integrated simply to find that the spreading radius of the rinsing liquid grows exponentially as $r_N' \sim r_o' e^{t'}$ where r_o' is the dimensionless radial position at the onset of exponential growth. Returning to dimensional form, denoted by the absence of a prime, gives

$$r_N \sim r_o e^{\Omega t}. \tag{3}$$

Remarkably, the simple approximation leading to Equation (3) predicts the observed exponential growth of the spreading radius. Further, it predicts the time constant of exponential growth of the spreading radius to be inversely proportional to the rotation rate. To evaluate this prediction, the time constant of each observation of exponential growth, τ, is calculated by fitting data between the initial splashing of the impinging liquid and the edge of the

substrate; then its inverse, τ^{-1}, is plotted in Figure 3b as a function of rotation rate. The high degree of correlation further supports this prediction; however, as an approximation, Equation (3) should not be expected to capture all complexities.

To demonstrate the robustness of this prediction, we seek a universal scaling of all rinsing experiments where exponential growth was observed. Figure 4a shows a plot of the azimuthally averaged spreading radius as a function of time for these experiments. When inspecting the data of a particular flow rate and rotation rate, nearly identical radial behavior between bare and SDS-coated substrates is observed. We hypothesize that the presence of SDS produces Marangoni stresses at the spreading front of the rinsing liquid, having a similar effect on spreading as the contact line of the bare substrate. When discussing water-coated substrates later, we will see that the absence of a contact line and Marangoni stresses substantially alters the spreading process. Figure 4b shows the same data with time scaled by Ω^{-1}, as found above, and radius by $(Q/2\pi l_{c,z}\Omega)^{1/2}$. This length scale emerges from matching the velocities due to flow and rotation rates, $Q/2\pi r_o l_{c,z} = \Omega r_o$. These scalings largely group the data within a narrow band before the edge of the substrate is reached. We postulate that an entirely singular response is not obtained due to the influence of the splashing of the impinging rinsing liquid on its initial dynamics on the substrate.

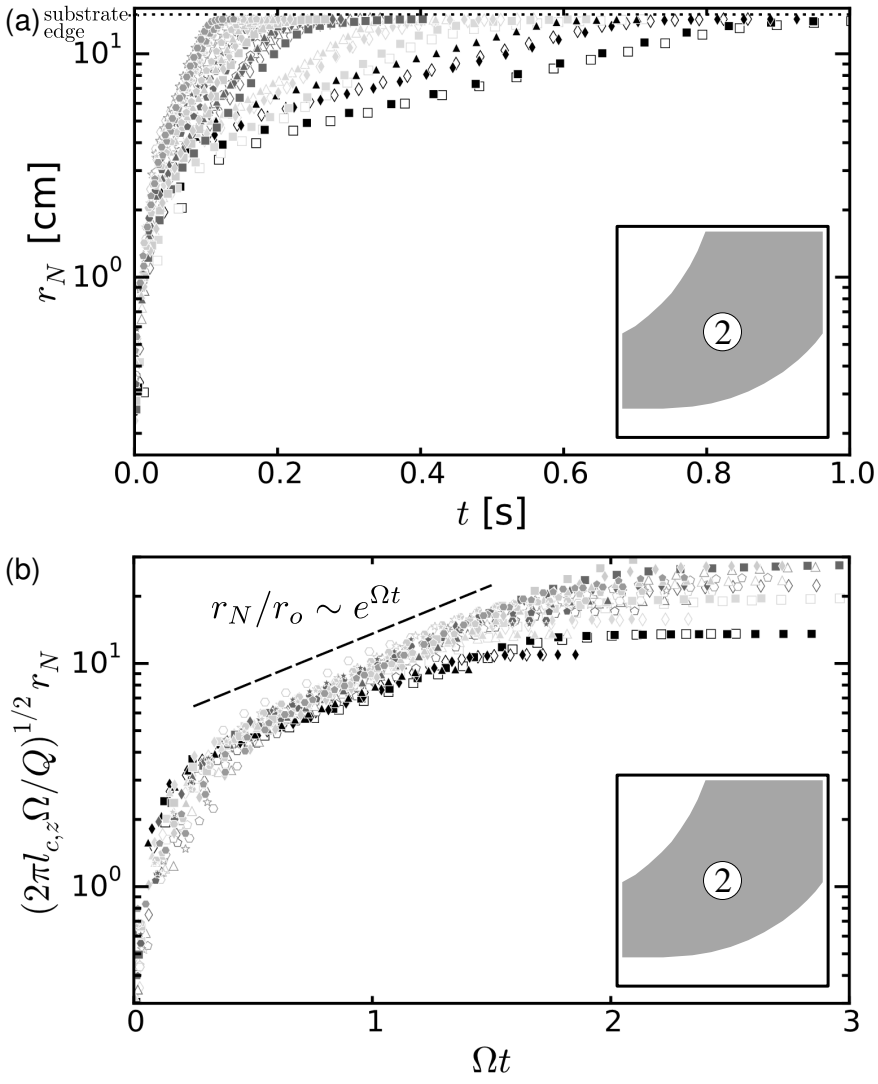

FIG. 4: (a) Plot of measurements of the azimuthally averaged spreading radii as functions of time for rinsing experiments where exponential growth was observed (Region 2). Symbol shapes indicate a particular flow rate as in Figure 3b. Colors ■, ■, ■, ■, and ■ indicate the rotation rate as 120, 250, 500, 750, and 1000 rev/min, respectively. Open and filled symbols indicate bare and SDS-coated substrates, respectively. The dotted line indicates the edge of the substrate. (b) Plot of the same data with radius and time scaled by $(Q/2\pi l_{c,z}\Omega)^{1/2}$ and Ω^{-1}, respectively. The dashed line indicates exponential growth.

Outside of Region 2, other growth rates of the spreading radius were observed. Figure 5 shows a plot of the azimuthally averaged spreading radius as a function of time for rinsing experiments of (a) Region 1 and (b) Region

3 on bare and SDS-coated substrates. The data are plotted on logarithmic axes, where a linear response indicates power-law behavior. Arrows indicate points in three experiments on bare substrates ((a) Q = 1290 mL/min, Ω = 0 rev/min; (b) Q = 840 and 1290 mL/min, Ω = 1000 rev/min) corresponding to the concentric outlines of the spreading fronts (insets). It is clear when comparing the concentric outlines across a consistent flow rate that the formation and frequency of rivulets is greatly pronounced in Region 3.

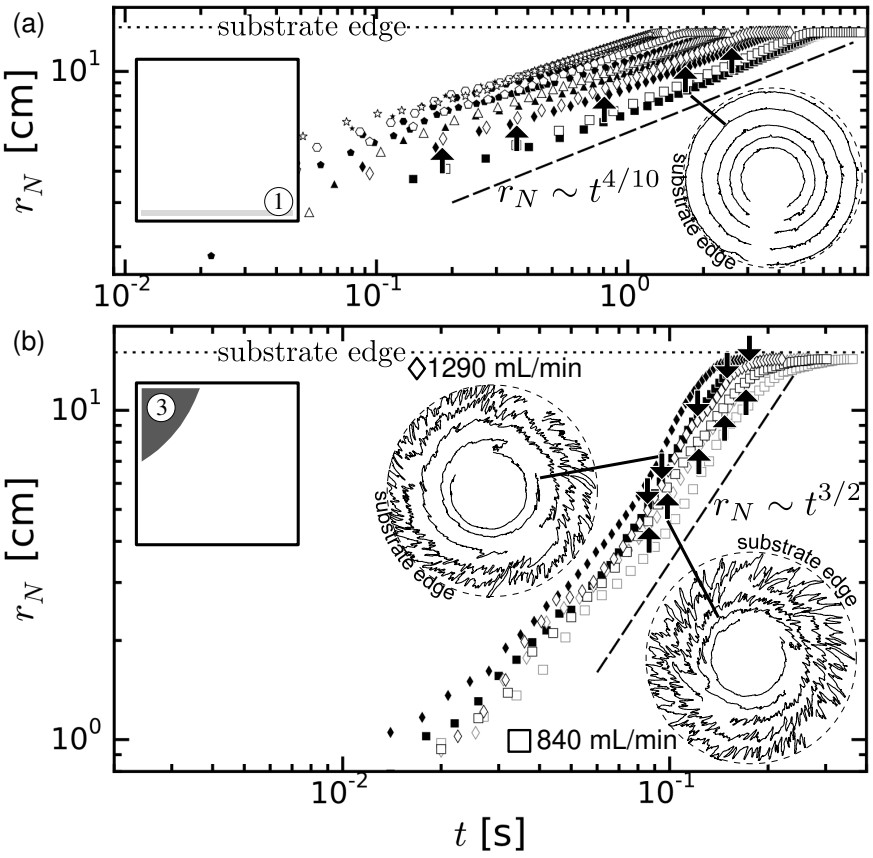

FIG. 5: Plots of measurements of the azimuthally averaged spreading radii as functions of time for rinsing liquids (water) spreading across bare and SDS-coated substrates from (a) Region 1 and (b) Region 3. Symbol shapes indicate a particular flow rate as in Figure 3b. Color ■ indicates the rotation rate as 0 rev/min in (a), and ■ and ■ indicate 750 and 1000 rev/min, respectively, in (b). Open and filled symbols indicate bare or SDS-coated substrates, respectively. Dashed and dotted lines indicate power laws and the edge of the substrate, respectively. Arrows indicate points in experiments on bare substrates ((a) Q = 1290 mL/min, Ω = 0 rev/min; (b) Q = 840 and 1290 mL/min, Ω = 1000 rev/min) corresponding to the concentric outlines of the spreading fronts (insets).

In Region 1 where the effect of rotation is small, Bond numbers of $O(10^{-3})$ indicate that capillarity dominates gravity in the spreading process [36]. Here, lubrication theory defines the height of a rinsing liquid spreading axisymmetrically due to capillarity with the dimensional evolution equation,

$$\frac{\partial h}{\partial t} + \frac{\sigma}{3\mu r}\frac{\partial}{\partial r}\left[rh^3\frac{\partial}{\partial r}\left(\frac{1}{r}\frac{\partial}{\partial r}r\frac{\partial h}{\partial r}\right)\right] = 0, \tag{4}$$

where σ is the surface tension of the rinsing liquid. A global continuity equation must also be specified, and its general form is

$$2\pi\int_0^{r_N(t)} rh(r,t)dr = Qt^\alpha, \tag{5}$$

where α is a constant that sets the the time dependence of the volume of spreading liquid. Setting α = 0 prescribes a constant volume, reflecting the work of Voinov [2], Tanner [3], and Cox [4], whereas setting α = 1 prescribes a constant flow rate, as in the case of the present rinsing experiments. A similarity solution [36] can be expressed using

a similarity variable, ξ, and the solution form of h

$$\xi = \left(\frac{\sigma Q^3}{3\mu}\right)^{-1/10} r t^{-(3\alpha+1)/10}, \tag{6}$$

$$h(r,t) = \xi_N \left(\frac{3\mu Q^2}{\sigma}\right)^{1/5} t^{(2\alpha-1)/5} \psi(\xi/\xi_N), \tag{7}$$

where ξ_N is the value of ξ at $r = r_N(t)$ and $\psi(\xi/\xi_N)$ is the similarity function, which transform Equations (4) and (5) into a single nonlinear ordinary differential equation in ψ that can be solved numerically or approximately; however, inspecting the similarity variable, ξ, reveals the time dependence of the spreading radius directly,

$$r_N(t) = \xi_N \left(\frac{\sigma Q^3}{3\mu}\right)^{1/10} t^{(3\alpha+1)/10}. \tag{8}$$

Choosing $\alpha = 0$ yields the commonly known Tanner's Law of $t^{1/10}$ for a constant volume spreading due to capillary forces [2–4], whereas the presently relevant $\alpha = 1$ provides the descriptive power law,

$$r_N \sim t^{4/10}, \tag{9}$$

of the data shown in Figure 5a. However, the prefactor of Equation (8) does not sufficiently collapse the data when used as a scaling, as the effect of splashing of the impinging rinsing liquid disturbs the initial condition on the substrate. Thus, the data is presented without any scaling for clarity.

Region 3 occurs above a threshold rotation rate that depends on, and increases with, the flow rate. Above a flow rate of 1740 mL/min, we no longer observed transitions into this region, as the threshold rotation rate exceeded the limit of our apparatus. The disappearance of exponential growth of the spreading radius and large increase in the frequency and aspect ratio of rivulets leads us to make two postulates to explain the data of Figure 5b obtained in this region: first, that the height of the rinsing liquid decreases substantially such that $\epsilon^2 Re \ll 1$, despite increasing Re; second, that the spreading of the rinsing liquid largely occurs down rivulets, and as rivulets break the axisymmetry of the spreading, approaches the behavior of two-dimensional flow driven by centrifugal forces, which gives the dimensional evolution equation

$$\frac{\partial h}{\partial t} + \frac{\Omega^2}{3\nu}\frac{\partial}{\partial x}\left(h^3 x\right) = 0, \tag{10}$$

where x and $x_N(t)$ are the lateral coordinate and length of a rivulet, respectively. Constructing the similarity variable, η, for Equations (10) and (5) gives the time dependence of the length of a rivulet driven by centrifugal forces as

$$x_N(t) = \eta_N \left(\frac{\Omega^2 A^2}{3\nu}\right)^{1/2} t^{(2\alpha+1)/2}, \tag{11}$$

where η_N is the value of η at $x = x_N(t)$ and A is the constant flow of rinsing liquid into a rivulet, the two-dimensional analog of Q. Setting $\alpha = 1$ to reflect the constant flow rate of the rinsing liquid yields a time dependence of

$$x_N \sim t^{3/2}. \tag{12}$$

We expect this relationship to serve as an upper bound for power-law growth as the increasing effects of rotation cause spreading of the rinsing liquid to increasingly occur through rivulets, as illustrated by their increasing aspect ratios. Equation (12) provides the descriptive power law of the data shown in Figure 5b. However, similarly to Figure 5a, the prefactor cannot collapse the data due to splashing of the impinging rinsing liquid and the data is presented without any scaling.

Within each of the three regions, we have explained the observed time-dependent spreading behavior on bare and SDS-coated substrates using lubrication theory. We now look to explain the boundaries that demarcate these regions from one another and the experiments that did not clearly reside within a particular region. In Figure 6, the observed time-dependent spreading behaviors of all experiments on bare and SDS-coated substrates are mapped onto the sketches of the three regions shown in Figure 2 with respect to the flow and rotation rates. Additionally, three theoretical boundaries are plotted that aim to explain the delineation of the experimental observations.

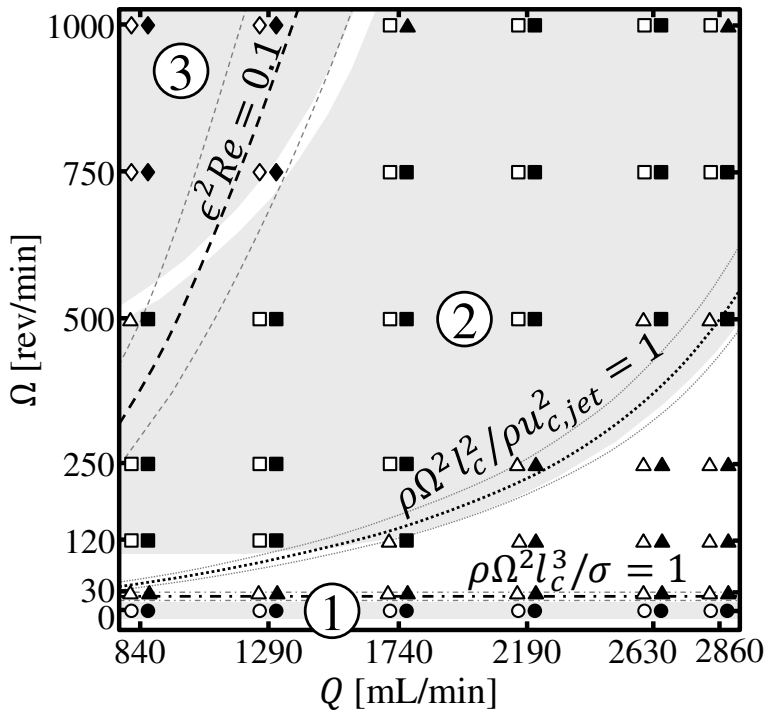

FIG. 6: A map of the experimentally observed spreading behavior on bare and SDS-coated substrates with respect to flow and rotation rates. Symbol shapes ○, □, ◇, and △ indicate the observed spreading behavior as capillary (power law), centrifugal (exponential), centrifugal (power law), or mixed, respectively. Open and filled symbols indicate bare or SDS-coated substrates, respectively. The dash-dotted lines indicate where the ratio between centrifugal and capillary forces, $\rho\Omega^2 l_c^3/\sigma$, is unity with three values of l_c chosen about the halfway point between the center and edge of the substrate: 7.0 cm (upper), 7.5 cm (middle, bold), and 8.0 cm (lower). The dotted lines indicate where the ratio between centrifugal forces and the inertia of the impinging jet, $\rho\Omega^2 l_c^2/\rho u_{c,jet}^2$, is unity with the characteristic velocity of the impinging jet, $u_{c,jet}$, chosen as $Q/2\pi l_c l_{c,z}$, l_c as above, and $l_{c,z}$ decreasing linearly from 500 to 150 μm across the range of flow rates. The dashed lines indicate where inertial terms of the lubrication equations become negligible, $\epsilon^2 Re = \Omega l_{c,z}^2/\nu = 0.1$, with $l_{c,z}$ chosen as $Qt_c/\pi l_c^2$, t_c as Ω^{-1}, and l_c as above. The three shaded areas are sketches of the three regions shown in Figure 2.

First, the dash-dotted lines indicate where the ratio between centrifugal and capillary forces, $\rho\Omega^2 l_c^3/\sigma$, is unity, which can be rearranged to give $\Omega = \sqrt{\sigma/\rho l_c^3}$. Three different values of l_c were chosen about the halfway point between the center and edge of the substrate: 7.0 cm (upper), 7.5 cm (middle, bold), and 8.0 cm (lower). The halfway point is a position on the substrate where it was observed that the rinsing liquid had consistently transitioned from its initial impingement behavior to its spreading behavior on the substrate. Three different values for l_c were chosen about this point to illustrate that the centrifugal force is a function of the radial position of the spreading front, and that estimates of where centrifugal forces overtake capillary forces are sensitive to this choice. These choices of characteristic lengths give similar values of rotation rate for the transition between capillary and centrifugal spreading, approximately 30 rev/min. With respect to Region 1, these lines fall along its experimentally observed upper boundary. With respect to Region 2, there is a gap between the theoretically predicted and experimentally observed lower boundary. At low flow rates, the gap is relatively small as compared to higher flow rates when the lower boundary of Region 2 trends upwards. A constant portion of this gap can be attributed to the transition between the two driving forces. For any non-zero rotation rate, there is some r where centrifugal forces dominate capillary forces. Thus, in the experiments conducted between Regions 1 and 2, mixed spreading behavior was observed where initially the rinsing liquid spread due to capillary forces at smaller values of r before spreading due to centrifugal forces at larger values of r. The increasing portion of this gap can be attributed to the increased inertia of the impinging jet of rinsing liquid at higher flow rates, which causes the rinsing liquid to propagate further radially on the substrate due its inertia, resulting in a mixed spreading behavior on the substrate and requiring a higher rotation rate to overcome this inertia at smaller radial positions to achieve a consistent spreading behavior across the entire substrate.

Thus, second, the dotted lines indicate where the ratio between centrifugal forces and the inertia of the impinging jet, $\rho\Omega^2 l_c^2/\rho u_{c,jet}^2$, is unity, with the characteristic velocity on the substrate due to the impinging jet, $u_{c,jet}$, chosen as $Q/2\pi l_c l_{c,z}$. Rearranging this ratio gives $\Omega = Q/2\pi l_c^2 l_{c,z}$. The same three values of l_c were chosen as above to illustrate that the centrifugal force and the velocity on the substrate due to the impinging jet are functions of the radial position of the spreading front, and that estimates of where centrifugal forces overcome the inertia from the

impinging jet are sensitive to this choice. As the depth of the fluid within a hydraulic jump decreases with increasing flow rate, we selected $l_{c,z}$ to decrease linearly across the range of flow rates as its simplest reflection. Specifically, 500 and 150 μm were selected as the values of $l_{c,z}$ at the minimum and maximum flow rate, respectively, such that this theoretical boundary aligns with the experimentally observed lower boundary of Region 2.

And third, the dashed lines indicate where $\epsilon^2 Re = \Omega l_{c,z}^2/\nu = 0.1$, signifying that inertia is negligible. By relating $l_{c,z}$ to l_c by global mass conservation, $l_{c,z} = Qt_c/\pi l_c^2$, and choosing t_c as Ω^{-1}, a parabolic relationship between the rotation and flow rates results: $\Omega = Q^2/\pi^2\epsilon^2 Re\nu l_c^4$. The same three values of l_c were chosen as above to illustrate that the centrifugal force is a function of the radial position of the spreading front, and that estimates of where inertia becomes negligible are sensitive to this choice. These three lines roughly align with the experimentally observed boundary between Regions 2 and 3, although the theoretical lines increase more sharply.

Our experimental observations and application of lubrication theory to describe the three time-dependent spreading behaviors on bare and SDS-coated substrates support the basis from which the three theoretical boundaries shown in Figure 6 arise. The ratio between capillary and centrifugal forces as the dominant spreading mechanism, which is the basis for the first theoretical boundary described, corresponded to the formation of rivulets in prior reports by Melo *et al.* [15] and Fraysse and Homsy [17]. Although we do not discuss rivulets explicitly in this paper, we reported in Ylitalo *et al.* [37] that rivulets were observed to varying degrees upon this ratio exceeding unity, which aligns with these prior reports. The primary distinction between Regions 2 and 3 is the observation of exponential spreading in the former, and of power-law spreading in the latter. By utilizing inertial lubrication theory, the exponential behavior was explained, while standard lubrication theory predicted the power-law behavior. The distinguishing feature between inertial and standard lubrication theory is the value of $\epsilon^2 Re$ and whether it is small enough to discard, which is the basis for the third theoretical boundary described. Secondarily, the rivulets that we observed in Region 3 had large aspect ratios, and here we postulated that the limiting behavior for the growth of rivulets with increasing aspect ratio was two dimensional flow down those rivulets. In Ylitalo *et al.* [37], we observed that the aspect ratio of rivulets increased with increasing rotation rate and decreasing flow rate, which is reflective of the location of Region 3 here.

An important consideration for a future study in constructing a rigorous phase diagram is the dependence of centrifugal force on radial position. As we stated, evident in the characteristic ratio of centrifugal forces to capillary forces, $\rho\Omega^2 r^2/(\sigma/h)$, is that every nonzero rotation has some corresponding radial position beyond which centrifugal force dominates. Coincidentally, a single spreading behavior was observed across the entire 300-mm-diameter substrate in most of our experiments, with each spreading behavior spanning a particular parameter space shown in Figure 6. However, for experiments conducted in the parameter spaces between and at the edges of these regions, we observed multiple spreading behaviors within a single rinsing experiment as the spreading transitioned from one region to another. On an infinite, or otherwise "large," substrate, and at a low rotation rate such that the centrifugal force rises more gradually across the substrate, each spreading behavior and the transitions between each could be observed over longer distances; we anticipate that a progression through all three regions could be observed in a single rinsing experiment while maintaining constant flow and rotation rates if experimental equipment can be designed appropriately. Alternatively, the rotation or flow rate could be cleverly modulated to maintain a particular spreading behavior over longer radial lengths: for example, by adjusting the rotation rate as a function of time to maintain a particular centrifugal force at the spreading front of the rinsing liquid ($\rho\Omega^2 r_N^2$ = constant), or the flow rate to maintain the mean thickness of the rinsing liquid as it spreads ($Qt = \pi r_N^2 h$).

On water-coated substrates, only power-law growth of the spreading radius was observed. Figure 7 shows a plot of the azimuthally averaged spreading radius as a function of time for a flow rate of 840 mL/min on a water-coated substrate at rotation rates spanning 0 to 1000 rev/min, and is representative of the observations at the other flow rates. The axes are logarithmic and three dashed lines indicate power laws. Two, $t^{4/10}$ and $t^{3/2}$, come from our analysis above. The third emerges from the similarity variable for the dimensional evolution equation for axisymmetric spreading due to centrifugal forces,

$$\frac{\partial h}{\partial t} + \frac{\Omega^2}{3\nu}\frac{1}{r}\frac{\partial}{\partial r}\left(h^3 r^2\right) = 0. \tag{13}$$

Constructing the similarity variable, ζ, for Equations (13) and (5) and rearranging it to solve for r_N gives

$$r_N(t) = \zeta_N \left(\frac{\Omega^2 Q^2}{3\nu}\right)^{1/4} t^{(2\alpha+1)/4}. \tag{14}$$

Setting $\alpha = 0$ gives the result obtained by Melo *et al.* [15] and Fraysse and Homsy [17] of $t^{1/4}$ for a constant volume spreading due to centrifugal forces, whereas the presently relevant $\alpha = 1$ provides the descriptive power law,

$$r_N \sim t^{3/4}. \tag{15}$$

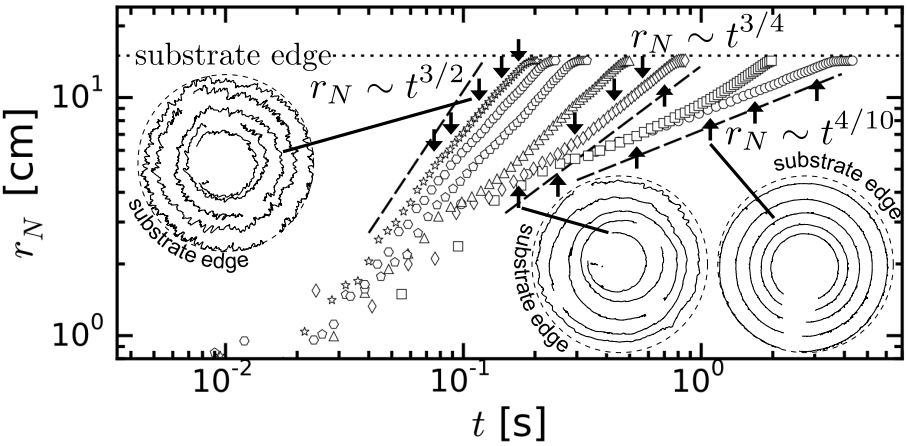

FIG. 7: Plot of measurements of the azimuthally averaged spreading radius as a function of time for rinsing liquids (water) spreading across water-coated substrates (Q = 840 mL/min, $0 \leq \Omega \leq 1000$ rev/min). Symbol shapes ○, □, ◇, △, ⬠, ⬡, and ☆ indicate the rotation rate as 0, 30, 120, 250, 500, 750, and 1000 rev/min, respectively. Dashed and dotted lines indicate power laws and the edge of the substrate, respectively. Arrows indicate points in experiments (Ω = 0, 120, and 1000 rev/min) corresponding to the concentric outlines of the spreading fronts (insets).

When the substrate is stationary, capillary forces dominate and the spreading radius expectantly grows following a power law of $t^{4/10}$. Increasing the rotation rate to 30 rev/min shows a transition between the power laws of $t^{4/10}$ and $t^{3/4}$ during spreading, reflecting the transition between the dominance of capillary and centrifugal forces. At 120 rev/min, the observed power law is again $t^{3/4}$. The power law of $t^{3/4}$ appears to be a distinct descriptor for a parameter region rather than simply a transitory rate, evident at both 30 and 120 rev/min, but warrants additional consideration in a future study. Further increases to the rotation rate yield a monotonic increase in the descriptive power law of the spreading radius, not quite reaching the power law of $t^{3/2}$ to the degree observed on bare and SDS-coated substrates shown in Figure 5b.

Thus, two notable differences emerged between spreading on a water-coated substrate and spreading on a bare or SDS-coated substrate. First, in the parameter space where exponential spreading was observed on bare and SDS-coated substrates, a monotonic transition between power laws was observed on water-coated substrates. And second, spreading on bare and SDS-coated substrates at high rotation rates and low flow rates more closely approached the power law of $t^{3/2}$, which emerged from lubrication theory when assuming that liquid spread two dimensionally down a rivulet due to centrifugal forces. We attribute both outcomes to the absence of a distinct contact line on a water-coated substrate. First, the absence of a distinct contact line reduces the height of the rinsing liquid near the spreading front such that inertia becomes negligible, eliminating the possibility of exponential growth of the spreading radius; indeed, estimating $\epsilon^2 Re = \Omega l_{c,z}^2/\nu$ with the coating thickness of 15 μm and the rotation rate at its maximum value of 1000 rev/min gives a value of 0.004. Even as the actual thickness of the spreading front is likely somewhat greater than the coating thickness, it is not until it is approximately fifteen times greater, at 250 μm, that $\epsilon^2 Re$ becomes $O(1)$. Second, the absence of a distinct contact line diminishes the advantage of a rivulet as a path of lower resistance to flow such that its aspect ratio is substantially reduced. This reduction is evident when comparing the outlines of the spreading fronts across coating conditions. Thus, the character of the spreading on bare and SDS-coated substrates at high rotation rates and low flow rates more closely approaches the assumptions that led to the power law of $t^{3/2}$.

IV. CONCLUSION

We conducted experiments to study the time-dependent spreading behavior of rinsing liquids across horizontal, rotating substrates, observing four distinct time-dependent behaviors for the growth of the spreading radius throughout the parameter space. Using lubrication theory, we explained the four observed time-dependent behaviors for the spreading radius, as well as defining theoretical boundaries to delineate each.

In the absence of rotation, or at small radial positions where centrifugal forces were comparatively small, the rinsing liquid was observed to spread following a power law of $t^{4/10}$, indicating capillary forces as the driving mechanism.

At larger rotation rates or radial positions where centrifugal forces were dominant, several behaviors were observed. On bare and SDS-coated substrates, centrifugal forces either led the spreading radius to grow exponentially with a time constant approximately equivalent to the rotation rate, or following a power law of $t^{3/2}$. The exponential

behavior emerged from inertial lubrication theory with centrifugal forces as the dominant spreading mechanism and axisymmetric coordinates to represent the axisymmetric character of the spreading, while the power-law behavior emerged from lubrication theory with centrifugal forces and two-dimensional coordinates to represent the large aspect ratio of the rivulets, down which the rinsing liquid largely spread. Interestingly, by assuming a coordinate system that reflected the character of the flow after the formation and growth of rivulets, we found that lubrication theory provided an adequate description of the time dependence of spreading with the power law of $t^{3/2}$, in contrast with other researchers who curtailed their use of lubrication theory once rivulets emerged. On water-coated substrates, no exponential growth was observed; rather, the time-dependent behavior of the spreading radius spanned between two power laws, $t^{3/4}$, emerging from lubrication theory with centrifugal forces as the dominant spreading mechanism and axisymmetric coordinates, and the aforementioned $t^{3/2}$.

Across bare and SDS-coated substrates, nearly identical radial behavior was observed, leading us to hypothesize that the presence of SDS produces Marangoni stresses at the spreading front of the rinsing liquid, having a similar effect on spreading as the contact line of the bare substrate; in contrast, the absence of a distinct contact line on a water-coated substrate reduced the height of the rinsing liquid near the spreading front such that inertia became negligible and exponential spreading was not observed; it also diminished the advantage of a rivulet as a path of lower resistance to flow.

In a companion paper by Ylitalo *et al.* [37], we discussed in detail the rivulets observed in these experiments, and their formation, growth, and morphologies.

V. ACKNOWLEDGEMENTS

The authors are grateful for funding from Lam Research, the Lam Foundation, NSF CBET Grant Nos. 1335632 (D.J.W., G.G.F.), and 1435683 (J.M.F., G.G.F.). We gratefully acknowledge the equipment support of Lam Research in constructing the apparatus. We would like to thank Prof. John Brady for a productive discussion regarding inertial lubrication.

*D.J.W. and A.S.Y. contributed equally to this work; †jfrostad@mail.ubc.ca; ‡ggf@stanford.edu.

[1] C. Huh and L. E. Scriven, Hydrodynamic model of steady movement of a solid/liquid/fluid contact line, J. Colloid Interface Sci. **35**, 85-101 (1971).
[2] O. V. Voinov, Hydrodynamics of wetting, Fluid Dyn. **11**, 714-721 (1976).
[3] L. H. Tanner, The spreading of silicone oil drops on horizontal surfaces, J. Phys. D **12**, 1473-1484 (1979).
[4] R. G. Cox, The dynamics of the spreading of liquids on a solid surface. Part 1. Viscous flow, J. Fluid Mech. **168**, 169-194 (1986).
[5] N. Didden and T. Maxworthy, The viscous spreading of plane and axisymmetric gravity currents, J. Fluid Mech. **121**, 27-42 (1982).
[6] H. E. Huppert, The propagation of two-dimensional and axisymmetric viscous gravity currents over a rigid horizontal surface, J. Fluid Mech. **121**, 43-58 (1982).
[7] A.-M. Cazabat, How does a droplet spread?, Contemp. Phys. **28**, 347-364 (1987).
[8] J.-F. Joanny and D. Andelman, Steady-state motion of a liquid/liquid/solid contact line, J. Colloid Interface Sci. **119**, 451-458 (1987).
[9] L. M. Pismen and J. Eggers, Solvability condition for the moving contact line, Phys. Rev. E **78**, 056304 (2008).
[10] A. Eddi, K. G. Winkels, and J. H. Snoeijer, Short time dynamics of viscous drop spreading, Phys. Fluids **25**, 013102 (2013).
[11] D. J. Walls, S. J. Haward, A. Q. Shen, and G. G. Fuller, Spreading of miscible liquids, Phys. Rev. Fluids **1**, 013904 (2016).
[12] D. J. Walls, E. Meiburg, and G. G. Fuller, The shape evolution of liquid droplets in miscible environments, J. Fluid Mech. **852**, 422-452 (2018).
[13] R. V. Craster and O. K. Matar, Dynamics and stability of thin liquid films, Rev. Mod. Phys. **81**, 1131-1198 (2009).
[14] A. G. Emslie, F. T. Bonner, and L. G. Peck, Flow of a viscous liquid on a rotating disk, J. App. Phys. **29**, 858-862 (1958).
[15] F. Melo, J.-F. Joanny, and S. Fauve, Fingering instability of spinning drops, Phys. Rev. Lett. **63**, 1958-1961 (1989).
[16] S. M. Troian, E. Herbolzheimer, S. A. Safran, and J.-F. Joanny, Fingering instabilities of driven spreading films, EPL **10**, 25-30 (1989).
[17] N. Fraysse and G. M. Homsy, An experimental study of rivulet instabilities in centrifugal spin coating of viscous Newtonian and non-Newtonian fluids, Phys. Fluids **6**, 1491-1504 (1994).
[18] M. A. Spaid and G. M. Homsy, Stability of Newtonian and viscoelastic dynamic contact lines, Phys. Fluids **8**, 460-478 (1996).
[19] M. A. Spaid and G. M. Homsy, Stability of viscoelastic dynamic contact lines: An experimental study, Phys. Fluids **9**, 823-832 (1997).

[20] S. K. Wilson, R. Hunt, and B. R. Duffy, The rate of spreading in spin coating, J. Fluid Mech. **413**, 65-88 (2000).
[21] I. S. McKinley, S.K. Wilson, and B. R. Duffy, Spin coating and air-jet blowing of thin viscous drops, Phys. Fluids **11**, 30-47 (1999).
[22] I. S. McKinley and S. K. Wilson, The linear stability of a drop of fluid during spin coating or subject to a jet of air, Phys. Fluids **14**, 133-142 (2002).
[23] K. E. Holloway, P. Habdas, N. Semsarillar, K. Burfitt, and J. R. de Bruyn, Spreading and fingering in spin coating, Phys. Rev. E **75**, 046308 (2007).
[24] T. T. Hsu, T. W. Walker, C. W. Frank, and G. G. Fuller, Role of fluid elasticity on the dynamics of rinsing flow by an impinging jet, Phys. Fluids **23**, 033101 (2011).
[25] T. W. Walker, T. T. Hsu, C. W. Frank, and G. G. Fuller, Role of shear-thinning on the dynamics of rinsing flow by an impinging jet, Phys. Fluids **24**, 093102 (2012).
[26] L. Rayleigh, On the theory of long waves and bores, Proc. Royal Soc. Lond. A **90**, 324-328 (1914).
[27] E. J. Watson, The radial spread of a liquid jet over a horizontal plane, J. Fluid Mech. **20**, 481-499 (1964).
[28] A. D. D. Craik, R. C. Latham, M. J. Fawkes, and P. W. F. Gribbon, The circular hydraulic jump, J. Fluid Mech. **112**, 347-362 (1981).
[29] R. I. Bowles and F. T. Smith, The standing hydraulic jump: Theory, computations and comparisons with experiments, J. Fluid Mech. **242**, 145-168 (1992).
[30] X. Liu and J. H. Lienhard, The hydraulic jump in circular jet impingement and in other thin liquid films, Exp. Fluids **15**, 108-116 (1993).
[31] F. J. Higuera, The hydraulic jump in a viscous laminar flow, J. Fluid Mech. **274**, 69-92 (1994).
[32] C. Ellegaard, A. E. Hansen, A. Haaning, K. Hansen, A. Marcussen, T. Bohr, J. L. Hansen, and S. Watanabe, Creating corners in kitchen sinks, Nature **392**, 767-768 (1998).
[33] K. Yokoi and F. Xiao, Relationships between a roller and a dynamic pressure distribution in circular hydraulic jumps, Phys. Rev. E **61**, R1016-R1019 (2000).
[34] J. W. M. Bush, J. M. Aristoff, and A. E. Hosoi, An experimental investigation of the stability of the circular hydraulic jump, J. Fluid Mech. **558**, 33-52 (2006).
[35] J. W. M. Bush and J. M. Aristoff, The influence of surface tension on the circular hydraulic jump, J. Fluid Mech. **489**, 229-238 (2003).
[36] L. G. Leal, *Advanced Transport Phenomena* (Cambridge, 2007).
[37] A. S. Ylitalo, D. J. Walls, D. S. L. Mui, J. M. Frostad, and G. G. Fuller, Evolution of rivulets during spreading of an impinging water jet on a rotating, pre-coated substrate, Phys. Fluids **31**, XXXXXX (2019).
[38] G. K. Batchelor, *An Introduction to Fluid Dynamics* (Cambridge, 1967).